Computational Fluid Dynamics of Hot Current from a Fire Source near a Tunnel Wall

OSAMU IMAZEKI[1], HITOSHI KURIOKA[2], YASUSHI OKA[3],
SHINICHI TAKIGAWA[3], and REIKO AMANO[4]
[1] I.T. Solution Department/ Kajima Corporation
6-5-30, Akasaka, Minato-ku, Tokyo, 107-8502, Japan
[2] Technical Research Institute/ Kajima Corporation
2-19-1, Tobitakyu, Chofu-shi, Tokyo, 182-0036, Japan
[3] Department of Safety Engineering/ Yokohama National University
79-5, Tokiwadai, Hodogaya-ku, Yokohama, 240-8501, Kanagawa, Japan
[4] Civil Engineering Management Division/ Kajima Corporation
1-2-7, Motoakasaka, Minato-ku, Tokyo, 107-8388, Japan

ABSTRACT

Numerical Simulation by CFD was carried out to understand the hot current behavior in a tunnel with longitudinal ventilation. It becomes clear that fire source modeling is very important because the hot current behavior is strongly affected by the fire source position and is sensitive to methods in the modeling of the fire source. The flame area which has developed from the fire source is an area of chemical reaction caused by combustion. Even if grids in the vicinity of the fire source are made fine, it was difficult to simulate the heat generation area with consideration to this chemical reaction through using a method for setting the heat release rate simply on the fire source surface. Therefore, we proposed a method adopting the knowledge on flame shape under the longitudinal ventilation and incorporating it into numerical simulation and it showed a good agreement with the experimental results. It was shown through experiments in a tunnel with longitudinal ventilation that the hot current developed toward the tunnel center downwind from the fire source near a wall. The cause was investigated by numerical simulation and it became clear from the results that the spiral air by the fire plume created a vortex in the crevice between the wall and the plume.

KEYWORDS: tunnel, fire, hot current, forced ventilation, fire source position, CFD

NOMENCLATURE LISTING

A_f	Fire area [$D_1 \times D_2$](m^2)	n	Number of rectangular elements in the heat release region
b	Tunnel opening width(m)	θ	Flame inclination angle (deg)
B_{max}	Maximum flame breadth(m)	q_i	Heat release rate of (i)th rectangular element in the heat release region(kW/m^2)
C_p	Specific heat(kJ/kg/K)	Q	Heat release rate of the fire source(kW)
D	Representative length(m)	Q^*	$Q/(\rho_a C_p T_a g^{1/2} D^{5/2})$
D_1	Fire source length in longitudinal direction(m)	Q^*_{DD1}	$Q/(\rho_a C_p T_a g^{1/2} D D_1^{5/2})$

FIRE SAFETY SCIENCE–PROCEEDINGS OF THE EIGHTH INTERNATIONAL SYMPOSIUM, pp. 1485-1496

D_2	Fire source length in a sectional direction (m)	Q^*_{DD2}	$Q/(\rho_a C_p T_a g^{1/2} DD_2^{5/2})$
DD_1	$D_2^{3/2}/D_1^{1/2}$(m)	R	Longitudinal distance from the center of fire source to the opening side (m)
DD_2	$D_1^{3/2}/D_2^{1/2}$(m)	S_i	Calorific area of (i)th rectangular element in the heat release region (m^2)
F_r	Froude number [$U_{wind}^2/g/H$]	T_a	Outside air temperature (K)
F_{rDD1}	Froude number [$U_{wind}^2/g/DD_1$]	ΔT	Rise in temperature from the initial temperature (K)
F_{rDD2}	Froude number [$U_{wind}^2/g/DD_2$]	ΔT_{max}	Maximum rise in temperature in vicinity of the ceiling (K)
g	Gravity acceleration (m/s^2)	t	Time (sec)
H	Height from a floor surface to a ceiling (m)	U_{wind}	Air supply wind speed (m/s)
L_{Bmax}	Position indicating the maximum flame breadth (m)	V_i	Volume of (i)th rectangular element in the heat release region (m^3)
L	Position indicating the rise to the maximum temperature [distance in a straight line from the center of fire source surface to the position indicating the rise to the maximum temperature directly under a ceiling] (m)	X_i	Virtual flame starting point on the floor (m)
		ρ_a	Air density (kg/m^3)

INTRODUCTION

Most of the studies on the flow behavior of fire plumes in a tunnel have been carried out by considering the spread of the hot currents under natural ventilation conditions on the assumption that the fire broke out at center of the tunnel in the sectional direction [1,2] or at the center of the lane [3,4] as well as the empirical formula describing the correlation between a longitudinal ventilated flow and a hot current. However, there has been little reporting on the hot currents in the case of the fire source being positioned near the wall. Two things were confirmed from the experiment carried out assuming that the fire broke out near the tunnel wall in the presence of longitudinal ventilation. One is that the position indicating the maximum temperature in the vicinity of the ceiling was shifted more downwind than that in the case of the fire source being placed at the center of the tunnel. The other is that the flame inclined toward the tunnel center downwind. Compared with the case of the fire source being placed at the center, when it is set near the wall it is feared that the specific hazard increases due to the expansion of the hot region downwind. Accordingly, the behavior of the hot currents in the case of the fire source being placed near the wall under longitudinal ventilation conditions was studied by carrying out a numerical simulation using CFD (Computational Fluid Dynamics). When investigating the hot currents in the proximity of the fire source using CFD, the fire source is modeled by setting the heat release rate as that on the fire source surface. However, it is difficult to reproduce the experiments in the area surrounding the fire source [5]. Due to the fact that in the hot current flow area subjected to the investigation in this paper, the flame inclined downwind because of the longitudinal ventilation, the

heat release region was modeled using the empirical flame shape prediction formulae [5,6] derived by the authors in place of the aforementioned modeling of the fire source in order to investigate and considered the reproducibility of the hot current behavior in the case of the fire source being placed near the wall under longitudinal ventilation. We proposed one method of CFD for improving the accuracy in reproducing experimental results even in the case of a little coarse grid surrounding the fire source.

EXPERIMENT OUTLINE

Figure 1 shows the schematic diagram of a 1/20 scale tunnel employed [7]. The dimensions of the tunnel are 0.6 m wide (X direction), 0.3 m high (Z direction) and 5.4 m (Y direction) long. An air flow was given uniformly in a longitudinal direction along the tunnel from its entrance on the air supply side. The ceiling and floor of the tunnel were made of steel plates with a thickness of 3 mm. The ceiling and the floor in the vicinity of the fire source is covered with heat insulating material made of ceramics fiber board with a thickness of 12.5 mm and this reduces heat loss. The side wall was made of fire resistant glass. The fire source was installed on the floor at a point 2.25 m away from the air supply opening of the entrance of the tunnel so that the position of fire source center could be b/8 (0.075 m: in the case of the fire source being placed near the wall) and b/2 (0.3 m: in the case of the fire source being placed at the center) away from the wall. Two different sizes of 0.1 m x 0.1 m for a square fire source and 0.3 m x 0.1 m for a rectangular fire source were established. The heat release rate was set at 0.4-18 kW and the ventilation velocity was set at 0-0.8 m/s. The burning time for the propane gas, which is employed as a fuel, was about 10 minutes. The experiments were carried out in 100 cases in all [5,8]. The temperature in the vicinity of the ceiling was measured at intervals of 2 sec using the thermocouples which were suspended in two lines in a position 10 mm under the ceiling, shown in Fig. 1. Thermocouples were arranged at 27 points in two lines at intervals of 0.05 m in the vicinity of the fire source ($r/H \leq 2$) and at intervals of 0.1-0.3m in the position far from the fire source ($r/H > 2$). Thermocouples in the vicinity of the fire source ($r/H \leq 3$) were also arranged to measure the maximum temperature at intervals of 0.05 m in the sectional direction of the tunnel (X-direction). The length of 0.05 m corresponds to the length of 1m in actual scale. When comparing the measured values with the computational results, the values obtained during a three minute period in the latter half of the burning time in which the temperature reached a quasi-steady state were used.

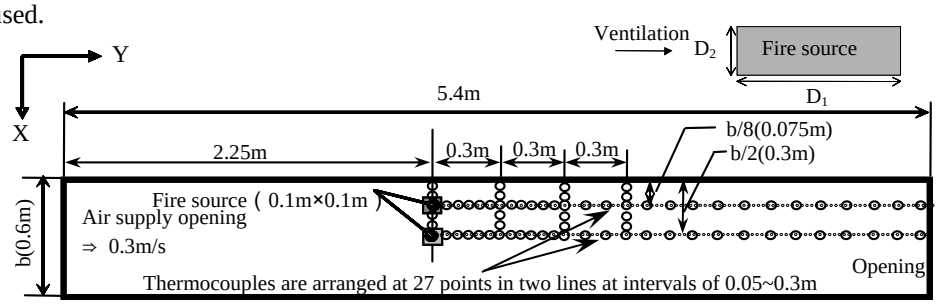

Fig. 1. Plane figure of the experiment tunnel model in a longitudinal direction.

EXPERIMENTAL RESULTS

Investigations into the temperature profile in the vicinity of the ceiling were carried out using the temperature data obtained under longitudinal ventilation conditions.

Temperature Profile in an Axial Direction along the Tunnel

A comparison of differences in the temperature profile due to the position of the fire source under longitudinal conditions is shown in Fig. 2. The maximum temperature appears at the position of r/H=1.5 due to the flame inclined by the forced ventilation. It was made clear that in the case of the fire source being placed near the wall the temperature of the ceiling at the center of the tunnel was higher than that of the ceiling along the central axis of the fire source at a location about 1m away downwind from the center of the fire source. It was also confirmed that the temperatures at the axes of b/2 and b/8 were distributed to a higher degree than those in the case of the fire source being placed at the tunnel center. It is thought that when the fire source was placed near the wall, with the shifting of the hot current to the downwind side, the hot region spread toward the tunnel center. This can be said from the observation of the fact that the flame inclined toward the tunnel center.

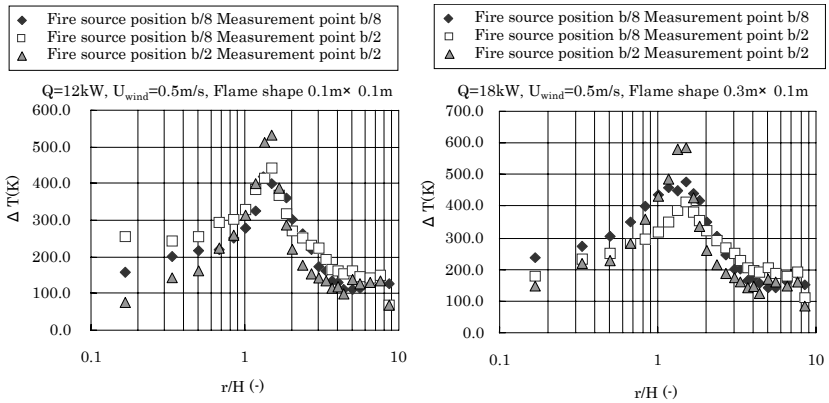

Fig. 2. Ceiling temperature profile under longitudinal ventilation.

Position Indicating Maximum Temperature of Fire Source Placed Near the Wall

Figure 3 shows the effects of the location of the fire source upon the position indicating the maximum temperature under longitudinal ventilation conditions. Symbols in Fig. 3 are plotted by changing the heat release rate to 4.5 KW, 9 KW and 12 KW as well as by changing the ventilation wind velocity to 0.3 m/s and 0.5 m/s in both cases of the fire source size being 0.1 m x 0.1 m and 0.3 m x 0.1 m. In the case of the fire source being paced near the wall (b/8), the position indicating the maximum temperature was seen on the downwind side rather than in the case of the fire source being placed at the tunnel center regardless of the fire source shape.

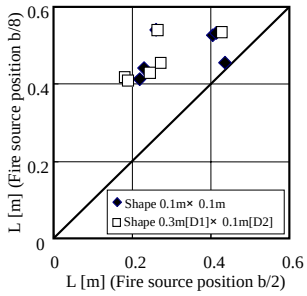

Fig. 3. Comparison of positions indicating maximum temperature at the ceiling.

NUMERICAL SIMULATION

The CFD code used in this study was the Fire Dynamics Simulator (referred to as the FDS [9]) developed by National Institute of Standard and Technology (NIST).

Computation Conditions

Table 1 explains the conditions used for the simulation. The simulation was carried out in the case of the ventilation wind velocity being considerably low, namely 0.3 m/s. The simulation was continued over 5 minutes by distributing the initial velocity and temperature uniformly to the computation cells in the tunnel. In this study, the wall was insulated in the same manner as that in the experiments. In order to notice similar phenomena in the area surrounding the fire source, as for the boundary conditions, the velocity component in y-direction on the air supply side was uniformly fixed at 0.3 m/s and on the opposite opening side the atmospheric pressure was set to be constant. The physical constants were determined with reference to the previous paper [10] and the same conditions as those for the experiments were given to the fire source. With regard to the lattice partitioning using an LES model, analyses should generally be carried out using an isotropic lattice. However, in the tunnel space the partitioning number of the lattice increases in a longitudinal direction. Therefore, in the computation the partitioning number of the lattice was established by reducing it in a range where analysis accuracy was not lowered based on the lattice partitioning described in the previous paper [5].

Table 1. Computation conditions.

Condition	Establishment
Initial condition	Velocity : 0m/s, Temperature: 22℃(Room temperature during measurement)
Wall condition	Velocity boundary:Half Slip[(a)], Heat boundary: Heat Insulation
Tunnel entrance boundary condition	Air supply opening: Fixed at 0.3m/s, Opening: Constant atmospheric pressure
Physical constant	Smagorinsky number=0.2, Prandtl number=0.8, Schmidt Number=0.5
Fire condition	Fuel: propane gas, Area: 0.1m×0.1m, Position: Floor, Q=4.5×t/60 (in case of t<60), Q=4.5(in case of $t \geq 60$)
Lattice partitioning	30(X-direction)×108(Y-direction)×15(Z-direction)

[(a)]When setting the velocity component of the virtual cell at UU and the velocity component of the cell opposite to the virtual cell with the boundary between at U, UU=1/2U.(under the condition that both UU and U are in parallel with the boundary)

Investigation of Establishment of Fire Source

Temperature Properties in the case of Centralized Fire Source

In general, when modeling the fire source in a simulation, an amount of fuel corresponding to the required heat release rate is supplied to the fire source surface (hereafter referred to as the centralized fire source). Figure 4 illustrates the result obtained from an actual measurement of the fire source section (b/8) in the case of the fire source being placed near the wall (b/8) and the simulation result. The position indicating the maximum temperature rise as a result of the actual measurement was discernible at Y=1H, but the computation result for the maximum temperature of the centralized fire source was seen at Y≒ 0.2H. It is thought that this was because the inclination of the gas which had not ignited yet due to the longitudinal ventilation was not accurately simulated. In this respect, fire source models need to be improved. When establishing the

fire source using a method in which the computation lattice in the vicinity of the fire source is partitioned into sections, the computation time increases. Accordingly, in order to simulate the temperature properties near the ceiling with the ordinary grid size used in this study, a simple prediction method in which the empirical formulae for flame shape prediction proposed by Kurioka [5] and Oka [6] was employed.

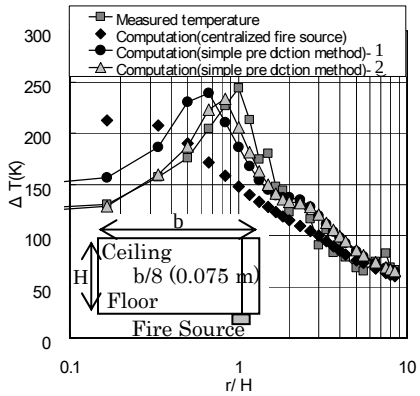

Fig. 4. Variation in temperature rise at the section (b/8) and at a position 10 mm directly under the ceiling by a centralized fire source simulation and by the simple prediction method simulation in the case of the fire source being placed near the wall (b/8).

Simple Prediction Method using Empirical Flame Shape Prediction Formulae

Due to the fact that the area subjected to the simulation is composed of rectangular meshes, it is necessary to make rectangular models using the flame shape computed by the empirical formulae for flame shape [5,6] and to distribute the amount of fuel corresponding to the required heat release rate to each rectangular element. Figure 5 shows the flow chart for the simple prediction method using the empirical formulae for flame shape. Equations 1-8 are empirical flame shape prediction formulae. Equation 5 and Eq. 7 are used in the case of the flame reaching the ceiling. Further, Eq. 6 and Eq.8 are used in the case of the flame failing to reach the ceiling. Table 2 [5] shows the coefficients for three regions classified according to the range of maximum rise in temperature($\Delta T_{\max}$) in the vicinity of the ceiling. The empirical flame shape prediction formulae were applicable to the tunnel space having the rectangular cross-section in a range of 1/3-1/1 for the aspect ratio under longitudinal ventilation conditions. These empirical formulae were obtained based on the experimental results carried out in the case of the fire source being placed at the center of a sectional direction of the tunnel. Figure 6 shows the variables used in the empirical flame shape formulae. As for the flame region defined by the empirical formulae for flame shape, the continuous flame region and intermittent flame region were modeled. In this paper, a region in which the temperature rose over 550 K was regarded as a chemical reaction region and a rectangular model of this heat release region was made. Through utilizing the relationship [5] between the fire plume breadth and the rise in temperature which was classified into a range where the temperature rose from the continuous flame region to the fire plume region, the boundary limits of the heat release region were obtained. Furthermore, with consideration to the fact that the region in which the chemical reaction finishes corresponds to the position indicating the maximum flame breadth (L_{Bmax}), the L_{Bmax} was employed for the length of the heat release region. In the simulation, on the assumption

that the heat release region is a cone composed of the fire source and the maximum flame breadth (B_{max}) as shown in Fig. 6, the heat release region was modeled by partitioning it into rectangular sections according to the rectangular mesh in the simulation region, Due to this, in this study the direction of the maximum flame breadth was established to be horizontal according to the rectangular mesh. The fuel was distributed to each section of the rectangular model using Eq. 9.

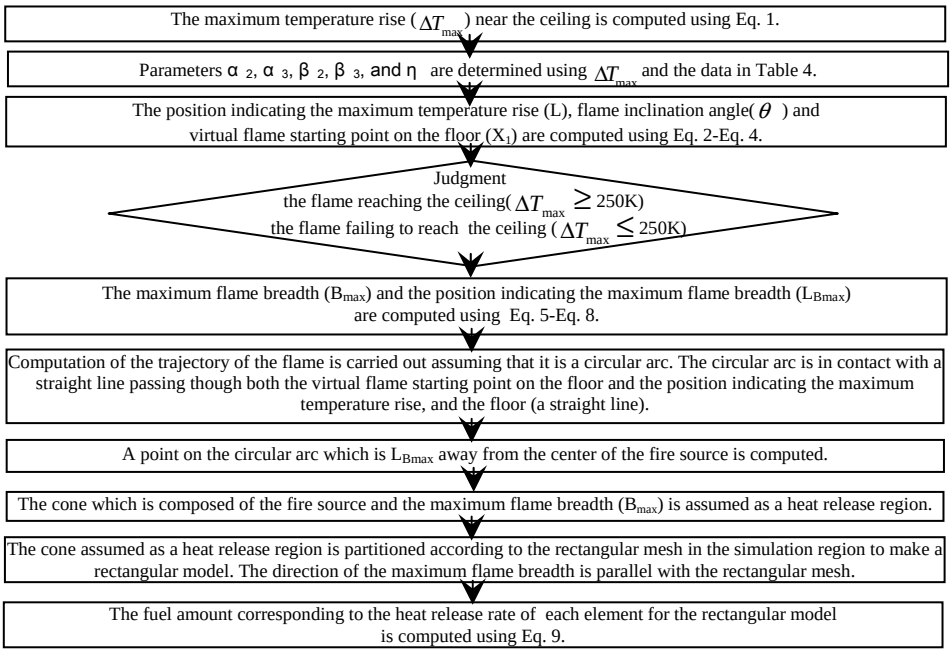

Fig. 5. Flow chart of simple prediction method using flame shape prediction equation.

$$\Delta T_{max} / T_a = \alpha_1 (K)^{\beta_1},\ K = Q^{*2/3} F_r^{-1/3} (b / D_2)^{1/2} \tag{1}$$

$$\alpha_1 = 0.6, \beta_1 = 1.2 \text{ (at } K < 3.3\text{)} \quad , \quad \alpha_1 = 2.53, \beta_1 = 0.0 \text{ (at } 3.3 \leq K < 8\text{)}$$

$$L(b / D_2)^{1/2} F_r^{1/2} / H = \alpha_2 [\, H^{3/2} b^{-1/2} A_f^{-1/2} Q^{*(2\eta-1)/5} \,]^{\beta_2} \tag{2}$$

$$\cos(\theta) F_r^{-1/2} = \alpha_3 [\, A_f^{1/2} b^{1/2} H^{-3/2} F_r^{-1} Q^{*(1-2\eta)/5} (b / D_2)^{1/2} \,]^{\beta_2} \tag{3}$$

$$X_1 = \sqrt{L^2 - H^2} - H \tan(\theta) \tag{4}$$

$$B_{max} / DD_2 = 0.68 (Q^*_{DD_2} / F_{rDD_2}^{1/6})^{2/5} \text{ (in case of the flame reaching the ceiling)} \tag{5}$$

$$B_{max} / DD_1 = 0.78 (Q^*_{DD_1})^{2/5} \text{ (in case of the flame failing to reach the ceiling)} \tag{6}$$

$$L_{Bmax} / DD_2 = 1.48(Q^*_{DD_2} / F^{1/6}_{rDD_2})^{2/5} \text{ (in case of the flame reaching the ceiling)} \quad (7)$$

$$L_{Bmax} / DD_1 = 1.43(Q^*_{DD_1})^{2/5} \text{ (in case of the flame failing to reach the ceiling)} \quad (8)$$

$$q_i = QV_i / [(\sum_{i=1}^{n} V_i) S_i] \quad (9)$$

Table 2. Parameter classification by ΔT_{max} .

Region	η	α_2	β_2	α_3	β_3
ΔT_{max} <250K(Plume Region)	-1/3	2.98	0.71	0.54	0.63
250K$\leq \Delta T_{max}$ <550K(Middle Region)	0	3.7	0.67	0.46	0.66
$\Delta T_{max} \geq$ 550K(Flame Region)	1/2	3.51	0.59	0.52	0.57

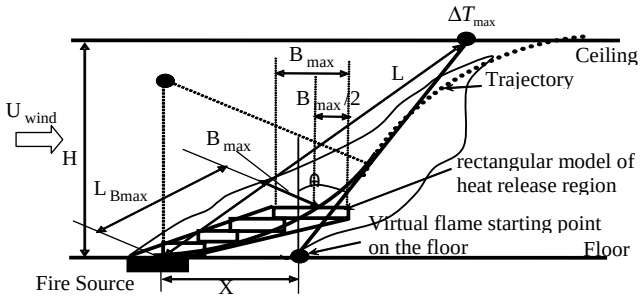

Fig. 6. Illustration of variables used in flame shape prediction formula and rectangular model of heat release region.

Establishment of Fire Source using Simple Prediction Method

The computation (simple prediction)-1 in Fig. 4 shows the results of the simulation carried out using the simple prediction method for the establishment of the fire source in the case of the fire source being placed near the wall (b/8). In the simulation, the position indicating the maximum temperature rise was seen at a point closer to the fire source than that obtained from the experiments. It is thought that this was caused by the fact that the empirical formulae for flame shape were derived from experiments in the case of the fire source being placed at the center in a sectional direction of the tunnel and that the flame shape in the case of the fire source being placed near the wall was different. Accordingly, the values of the flame inclination angle (θ), the maximum flame breadth (B_{max}) and the position indicating the maximum flame breadth (L_{Bmax}) were taken from the measurement results in the case of the fire source being placed near the wall. The computation (simple prediction)-2 in Fig. 4 shows the results obtained by carrying out computations again based on these values.

The aforementioned modification resulted in obtaining the position indicating the rise to the maximum temperature as well as the temperature properties in other regions which was approximate to the actual measurement results. Figure 7 illustrates the actual measurement result and the result by the simple prediction method simulation in the case of the fire source being placed at the center (b/2) in a sectional direction of the tunnel. The computational result showed a good agreement with the actual measurement result.

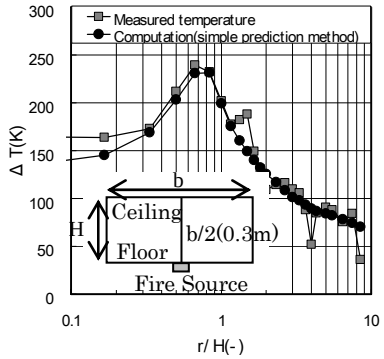

Fig. 7. Variation in temperature rise at section (b/2) and that obtained using the simple prediction method simulation at a position 10 mm directly under the ceiling in the case of the fire source being placed at the center (b/2) in a sectional direction of the tunnel.

EXPERIMENT RESULTS OF FIRE PERFORMANCE

Air Current Behavior

It was confirmed in the fire experiments carried out when the fire source was placed near the wall that with the spread of the flame which inclined due to the longitudinal ventilation toward a downwind side, the flame leaned toward the tunnel center away from the wall. So, the air current behavior in the tunnel section in the case of the fire source being placed near the wall (b/8) is examined from the results of the CFD simulation using the empirical formulae for flame shape. Figure 8 shows the behavior of the air flowing in a crevice section (b/15) between the fire source and the wall in the vertical section in a longitudinal direction. Air vortexes are generated at the space between Y1(Y=0.5H) and Y2(Y=1H) on the downwind side of the fire source. Figures 9 and 10 show the air current behavior in the vertical section in a sectional direction at Y1 and Y2 shown in Fig. 8.

It is confirmed from Fig. 9 that the ascending air current flowing toward the ceiling is the main current and that at the lower part close to the wall (part B) an air vortex is generated due to the spiral air current. At the central part (part C), an air vortex which is thought to be generated by the fire plumes is also confirmed. Figure 10 shows that a vortex generated near the wall (part D) becomes a spiral air current which develops in fire plumes and that as a result the center of the vortex generated at the central part (part E) lies a little toward the center in a sectional direction. It is thought that this is so because the spiral air current directs the fire plumes toward the tunnel center. It is also thought that the fire plume induced spiraling air which became a 3-dimensional air vortex (in horizontal and vertical directions) spread in the crevice between the fire plumes and the

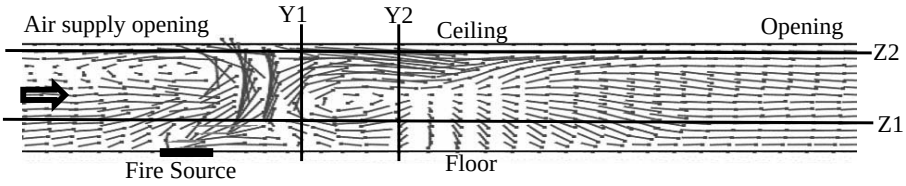

Fig. 8. Air flow in a longitudinal direction (Y- Z section)
crevice between fire source and wall (b/15).

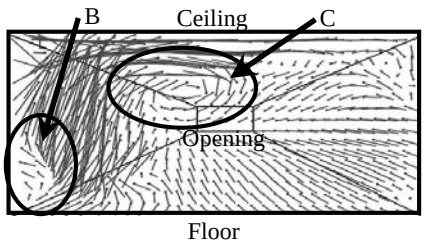

Fig. 9. Air flow in a sectional direction (X-Z section) Y1 section.

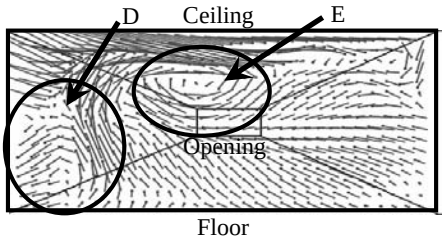

Fig. 10. Air flow in a sectional direction (X-Z section) Y2 section.

wall and created the phenomenon where the flame inclined toward the tunnel center on the downwind side.

Behavior of Temperature

Figure 11 and Fig. 12 show the temperature rise profile on the fire source section in the longitudinal direction (Y-Z section) both in the case of the fire source being placed near the wall (b/8) and in the case of it being placed at the center. The high temperature layer (A layer in which the temperature rises to 40 K or more is defined as a high temperature layer in this paper.) became thicker in a range of $r \geq 3H$ than in the case of the fire source being placed near the wall.

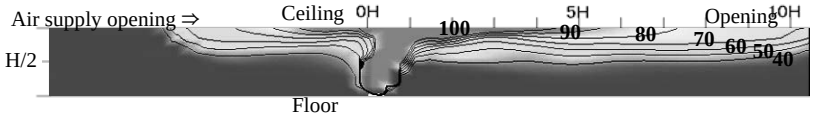

Fig. 11. Fire source section (b/2) temperature rise profile in the case of the fire source being placed near the wall (b/8) in a longitudinal direction (Y- Z section).

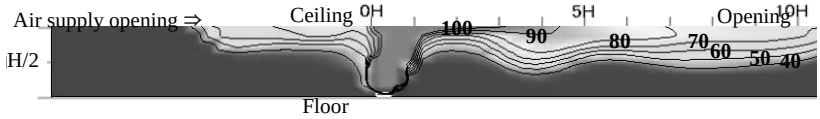

Fig. 12. Fire source section (b/2) temperature rise profile in the case of the fire source being placed at the center (b/2) in a longitudinal direction (Y- Z section).

In order to investigate the cause, the mass flow rate caused by the velocity component (U) in the sectional direction and by the velocity component (W) in a vertical direction is shown in Fig. 13. Figure 14 shows the mass flow rate caused by the velocity component (V) in a longitudinal direction. The values for the mass flow rate were obtained from the high temperature layer of the tunnel section in a sectional direction (X-Z). Figure 13 shows that in the vicinity of the position indicating the rise to the maximum temperature (Y=1H), the mass flow rate was high due to a great amount of spiraling air caused by the fire plumes both in the case of the fire source being placed near the wall and in the case of it being placed at the center. Moreover, the mass flow rate in the case of the fire source being placed at the center was higher than that in the case of the fire source being placed near the wall. However, it is clear that in the region of Y>2H, the mass flow rate caused by U and W for the velocity component was low. On the other hand, it is clarified in Fig. 14 that the mass flow rate caused by the velocity component (V) in the longitudinal direction in the case of the fire source being placed at the center was higher than that in

the case of the fire source being placed near the wall. In the region of Y>2H, the mass flow rates in both cases became almost constant. With consideration to these phenomena, it is deduced that regardless of the position of the fire source the mass flow rate of the spiral air current induced by the fire plumes in the space between the fire source and the ceiling has a great effect upon the high temperature layer. In the case of the fire source being placed near the wall, the amount of spiraling air when the fire plumes extended was smaller than the amount in the case of the fire source being placed at the center. Therefore, it is thought that the buoyancy of the high temperature layer was preserved and that the high temperature layer became not as thick on the downwind side as in the case of the fire source being placed at the center. On the other hand, it is also thought that in the case of the fire source being placed at the center, due to the fact that the amount of the fire plume induced spiraling air conveyed toward the high temperature layer at the upper part of the tunnel increased, the high temperature layer in the vicinity of the ceiling became thick because of the heat of dilution.

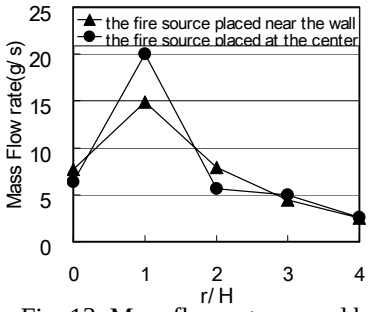

Fig. 13. Mass flow rate caused by the sectional velocity component (U) and vertical velocity component (W) in the case of the temperature rise $\geq$ 40 K.

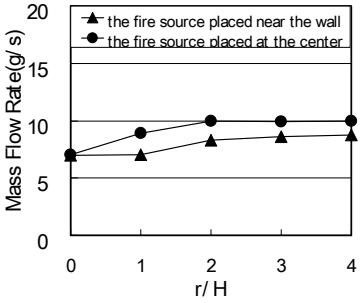

Fig. 14. Mass flow rate caused by the longitudinal velocity component (V) in the case of the temperature rise $\geq$ 40 K.

CONCLUSIONS

From the comparison between the experimental results and the computational results, the following conclusions were obtained.

- The position indicating the maximum temperature rise under longitudinal ventilation conditions when the position of the fire source was shifted to a place near the wall was more discernible on the downwind side than when the fire source was placed at the center. There was a tendency in which the high temperature region was directed toward the center.
- When substituting a rectangular model for the heat release region using the simple prediction method with the empirical formulae for flame shape in the case of the fire source being placed at the center under longitudinal ventilation conditions, the computation results agreed quite well with the measured results.
- In the case of the fire source being placed near the wall under longitudinal ventilation conditions, the position indicating the maximum temperature rise obtained from the simple prediction method using the empirical formulae for flame shape was seen at a point nearer to the fire source than that obtained from the measured results. When substituting a rectangular model for the flame shape obtained from the measurement values, it was confirmed that the computation results agreed with the measured results to a high degree. When carrying out computational

work using the simple prediction method in future, a simple model for predicting flame shape in the case of the fire source being placed near the wall will be necessary.

- When the fire source is placed near the wall under longitudinal ventilation conditions, the hot air current flows toward the downwind center. It is thought that this is so because the fire plume induced air current generated a vortex in the space between the wall and the fire plumes.
- The amount of spiraling air in case of the fire source being placed near the wall is smaller than the amount of spiraling air in the case of the fire source being placed at the center under longitudinal ventilation conditions. Accordingly, the high temperature layer at the upper part of the tunnel is preserved on the downwind side. This is thought to exert great effects on the surrounding space. Furthermore, when the fire source is placed at the center, the high temperature layer becomes thicker on the downwind side than when the fire source is placed near the wall. With regard to this, it is recommended that serious consideration be given to planning for evacuation and rescue activities.

REFERENCES

[1] Kawabata, N., Kunikane, Y., Yamamoto, N., Takekuni, K., and Shinoda, A., "Numerical Simulation of Smoke Descent in a Tunnel Fire," *Tunnel Management International*, **6**, (4), (2003).

[2] Kunikane, Y., Kawabata, N., Takekuni, K., and Shinoda, A., "Heat Release Rate in a Large Cross Section Tunnel," *Tunnel Management International*, **6**, (3), pp. 22-29, (2003).

[3] Woodburn, P.J., and Britter, R.E., "CFD Simulation of Tunnel Fire-Part1," *Fire Safety Journal*, **26**, pp. 35-62, (1996).

[4] Lea, C.J., "Computational Fluid Dynamics Simulations of Fires in Longitudinally-Ventilated Tunnel," HSL Report No.IR/L/FR/94/10, 1995.

[5] Kurioka, H., "Experimental Study on the Fire Safety in Tunnel Space," Doctoral thesis, 2003 [in Japanese].

[6] Oka, Y., Kurioka, H., Satoh, H., and Ogawa, T., "Effect of Fire Source Shape and its Size to Fire Phenomena in Tunnels," *Proceedings of the Symposium on Underground Space*, Vol. **9**, 2004, pp. 19-28, (in Japanese).

[7] Takigawa, S., Oka, Y., Kurioka, H., Satoh, H., Ikegami, K., and Fukuda, S., "Influence of Fire Source Position to Temperature Property of Ceiling Jet in Tunnel," *Annual Meeting of Japanese Association for Fire Science and Technology*, 2004, pp. 384-387 (in Japanese).

[8] Kurioka, H., Oka, Y., Satoh, H., and Sugawa, O., "Fire Properties in near Field of Square Fire Source with Longitudinal Ventilation in Tunnels," *Fire safety Journal*, **38**, (4), pp. 319-340, (2003).

[9] McGrattan, K.B., Baum, H.R., Rehm, R.G., Hamins, A., Forney, G.P., Floyd, J.E., Hostikka, S., and Prasad, K., "Fire Dynamics Simulator (Version3) Technical Reference Guide," NISTIR6783, 2002.

[10] Satoh, H., Kurioka, H., Imazeki, O., and Tanaka, F., "Computational Fluid Dynamics Simulation of Thermal Behavior under Working Water Screens in the Tunnel," *Proceedings of the Symposium on Underground Space*, Vol. **9**, 2004, pp. 69-78, (in Japanese).